Palaeogeography, Palaeoclimatology, Palaeoecology 293 (2010) 76–89

Contents lists available at ScienceDirect

Palaeogeography, Palaeoclimatology, Palaeoecology

journal homepage: www.elsevier.com/locate/palaeo

Trace-elemental derived paleoceanographic and paleoclimatic conditions for Pleistocene Eastern Mediterranean sapropels

D. Gallego-Torres [a,d,*], F. Martinez-Ruiz [b], G.J. De Lange [a], F.J. Jimenez-Espejo [c,b], M. Ortega-Huertas [d]

[a] Faculty of Geosciences, Utrecht University, The Netherlands
[b] Instituto Andaluz de Ciencias de la Tierra (CSIC-UGR), Spain
[c] Institute for Research on Earth Evolution, JAMSTEC, Japan
[d] Departamento de Mineralogía y Petrología, Universidad de Granada, Spain

ARTICLE INFO

Article history:
Received 8 February 2010
Received in revised form 29 April 2010
Accepted 1 May 2010
Available online 10 May 2010

Keywords:
Sapropel
Trace elements
Redox conditions
Sedimentary regime

ABSTRACT

Eastern Mediterranean sediments are characterized by cyclic deposition of organic-rich sediments known as sapropels. Enhanced primary productivity combined with bottom water oxygen depletion are thought to be the main drivers for sapropel deposition. We selected sapropel layers from a suite of ODP-Leg 160 cores, and applied a set of geochemical proxies to determine paleo-productivity variations, redox conditions of the water column during deposition, and provenance of detrital material.

High sedimentary Ba/Al and C_{org} contents indicate enhanced primary production, whereas the sedimentary La/Lu ratio, points to an enhanced contribution from a North African riverine source, during sapropel formation. These features are especially pronounced on Sapropels S5 and S7, deposited during a particularly warm climatic interval. This indicates a more intense North African drainage/weathering and consequently run-off for those sapropels that have the most enhanced expression of productivity too. Correspondingly, the latter has also resulted in bottom water redox conditions that have been more severe during these sapropels than during others.

Deepwater formation from Adriatic and Aegean areas, thought to be mainly controlled by sustained cooling of preconditioned surface waters, triggers the onset of bottomwater ventilation, thus sapropel duration. Our data, therefore, suggest that the intensity of sapropel formation is determined by the North African monsoonal system, whereas their duration is directed by northern borderlands climatic conditions.

1. Introduction

Eastern Mediterranean sediments consist of cyclic organic-rich and organic-lean deposits. Some of the Pleistocene organic-rich intervals (sapropels) are highly enriched in organic matter (e.g. Olausson, 1961; Cita et al., 1977; Kidd et al., 1978; Emeis et al., 1991). The link of these deposits to climate cycles, and particularly the control of astronomical precessional cycles has been reported (e.g., Rossignol-Strick, 1985; Hilgen, 1991) and is widely accepted. Two distinct interpretations for oceanographic conditions that resulted in sapropel formation have been suggested: 1. Water column stratification and anoxic bottom water resulting from a more sluggish circulation (e.g., Thunell et al., 1984; Rohling and Hilgen, 1991; Menzel et al., 2002; Negri et al., 2003; De Lange et al., 2008), and 2. Increased productivity and carbon burial (e.g., Calvert and Pedersen, 1993; Diester-Haass et al., 1998; Martinez-Ruiz et al., 2000; Weldeab et al., 2003; Meyers and Arnaboldi, 2005). These scenarios are not mutually exclusive, in fact a combination of both seems most plausible (e.g., De Lange and Ten Haven, 1983; Calvert et al., 1992; Nijenhuis and De Lange, 2000; Rinna et al., 2002; Filippelli et al., 2003; Slomp et al., 2004; Gallego-Torres et al., 2007). Increased export production would have induced greater oxygen consumption in deep waters resulting in anoxic conditions at and even above the sediment–water interface which would further promote organic matter preservation. Clearly, the relative contribution of the two endmember scenarios may not have been constant through time (e.g., Emeis et al., 1991; Passier et al., 1999; Martinez-Ruiz et al., 2003; Menzel et al., 2003). At the same time, from the spatial point of view, regional variations in sapropel expression have also been reported (e.g., Nijenhuis and De Lange, 2000; Nijenhuis et al., 2001 e.g., Arnaboldi and Meyers, 2006). Important differences within the pelagic environment may relate to basin dynamics and the intensity of the main deepwater circulation which induce spatial variations linked to sediments and nutrient distribution across the basin. All of these may not only result in variability among deepwater sapropels, particularly in relation to the conditions prevailing at the moment of sapropel onset and termination, but these may also affect the "intensity" of the sapropel event.

* Corresponding author. Departamento de Mineralogía y Petrología, Universidad de Granada, Spain.
E-mail addresses: davidgt@ugr.es, d.gallego@geo.uu.nl (D. Gallego-Torres).

0031-0182/$ – see front matter © 2010 Elsevier B.V. All rights reserved.
doi:10.1016/j.palaeo.2010.05.001

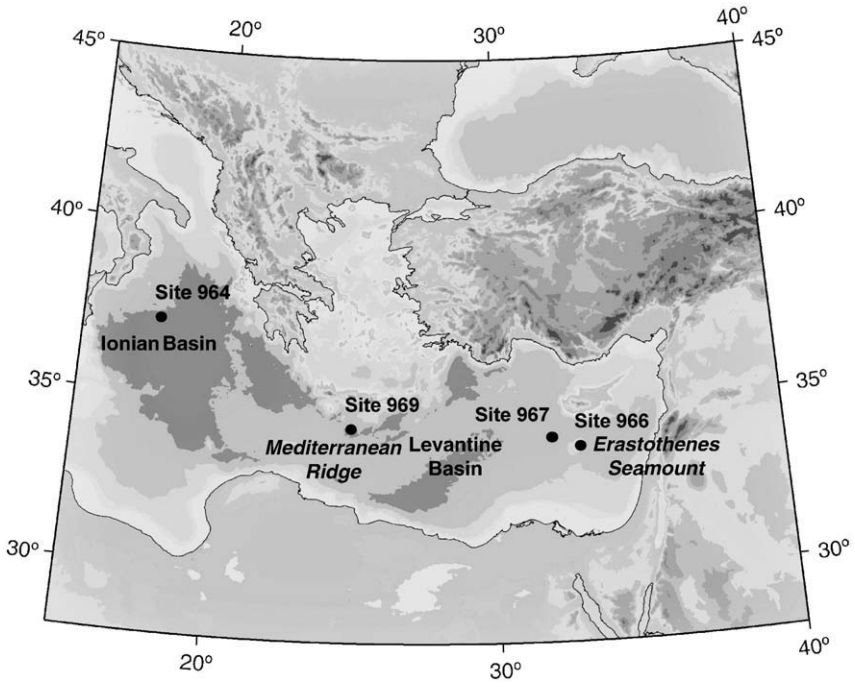

Fig. 1. Location map for the 4 studied sites. Site 964 (Lonian basin) is the deepest studied location. 966 is located on a polagic high, the Erathostenes seamount (see text details).

Timing and synchronicity for the onset and duration of sapropel formation is still debated. For all but the most recent sapropel, assumptions have to be made for the ages of the sapropel interval relative to astronomical (precession) cycle/summer insolation intensity or for the sedimentation rates during sapropel and non-sapropel periods (e.g., Van Os et al., 1994; Nijenhuis and De Lange, 2000; Capotondi et al., 2006). The exact oceanographic and climatic conditions that must have induced onset and termination of sapropel formation are another incompletely resolved issue. Enhanced river discharge from the Nile has been suggested as a driver for stratified water column conditions and for enhanced nutrient supply, thus primary productivity (e.g., Rossignol-Strick, 1985; Martinez-Ruiz et al., 2000), but variations in the Eastern Mediterranean circulation pattern are also expected to have played a role. Water depth and other local conditions have been reported to influence the sapropel expression in different locations (e.g., Murat and Got, 2000; Nijenhuis et al., 2001 e.g., Meyers and Arnaboldi, 2005; De Lange et al., 2008).

The aim of this paper is to clarify some of these uncertainties while focusing on a set of 4 sites drilled during ODP-Leg 160 that represent a transect across the Eastern Mediterranean basin. In addition, these four locations include the most representative settings in the basin, covering the areas of (1) influence from the northern margin, (2) Nile River dominance, (3) a pelagic high and (4) a central location within the Eastern Mediterranean basin (Fig. 1 and Table 1). The study includes several sapropel units from each site that represent the temporal evolution of sedimentary conditions at the time of sapropel formation.

The tools applied to reconstruct these conditions are a set of geochemical data used as proxies: Ba/Al as productivity (e.g., Bishop, 1988; Dymond et al., 1992; Van Os et al., 1994; Paytan, 1997); U, V, Mo to assess relative redox conditions (e.g., Wignall and Myers, 1988; Nijenhuis et al., 1999; Tribovillard et al., 2006; Gallego-Torres et al., 2007); in particular U_{aut}, and V/Mo have been applied for a semiquantitative evaluation of redox conditions (Jones and Manning, 1994; Piper and Calvert, 2009). In addition, Mn/Al ratio has been used to evaluate post-depositional oxidation (e.g., De Lange et al., 1989; Thomson et al., 1995; van Santvoort et al., 1996; Crusius and Thomson, 2003); and Hf/Zr and La/Lu ratios have been applied to assess the potential origin of terrigenous material (Hamroush and Stanley, 1990; Piper and Calvert, 2009). Combining all information, we will assess the environmental conditions that characterize sapropel events.

2. Material and methods

A transect of cores across the Eastern Mediterranean has been studied using samples recovered during ODP-Leg 160. We selected four locations representing different paleoceanographic environments (Fig. 1). Site 964 is located in a deep marine setting (3658 mbsl) on the Pisano Plateau (Ionian Basin), and is influenced by the Adriatic Sea and currents coming from the Western

Table 1
Location, ages (sapropel mid points, from Emeis et al., 2000) and correlation of studied sapropels. Shaded squares correspond to sampled sapropels.

Sapropel	i-cycle	Age	Site 964 3658 (mbsl) Pissano Plateau	Site 969 2200 (mbsl) Mediterranean Ridge	967 2555 (mbsl) Levantine Basin	966 926 (mbsl) Eretosthenes Seamount
S1	2	8 ky				
S5	12	124 ky				
S6	16	172 ky				
S7	18	195 ky				

Table 2
Summary of (A) calculated Linear Sedimentation Rates based on previously published ages on sapropel onset and termination, and (B) calculated ages based on constant LSRs between adjacent sapropel intervals, assuming 21 ky cycles.

A			Linear sedimentation rates (cm/ky)			
	Age (ky)		Site 964	Site 969	Site 967	Site 966
		Above	11.23[a]	2.98	18.42[a]	2.8
S1	9,8/5,7[b]		4.14	4.39	5.363	3.9
		Below	7.17	2.24	2.74	2.72
		Above	4.823	5.029		2.5
S5	124/119[c]		3.6	4.4		2.8
		Below	5.32	2.782		2
		Above	5.32	1.59	3.909	1.978
S6	176/170[d]		9.8	5.83	8.333	5.416
		Below	5.2	2.2	6.933	1.294
		Above	5.2	2.2		1.2
S7	197/191[d]		2	4.666		4.41
		Below	3.437	2.437		2.393

B	Ages							
	Site 964	LSR	Site 969	LSR	Site 967	LSR	Site 966	LSR
Top	7.15		5.10		7.16		6.00	
S1 (mid point)	8.00	9.38	8.00	3.5	8.00	14.75	8.00	4
Base	8.85		10.32		8.70		10.00	
Top	122.74		120.93				120.60	
S5 (mid point)	124.00	5.93	125.18	4.24			124.00	2.35
Base	125.76		126.12				126.55	
Top	168.01?		164.74		166.65		164.48	
S6 (mid point)	172.00	6	172.00	2.62	172.00	4.67	172.00	2.19
Base	175.15		178.11?		177.35		179.30	
Top	193.52		189.33				188.76	
S7 (mid point)	195.00	4.04	195.00	2.64			195.00	2.24
Base	196.48		199.91				200.58	

All depths considered from Emeis et al., 2000; Sakamoto et al., 1999.
[a] Slumped sediments (see text for details).
[b] Based on De Lange et al., 2008.
[c] Based on Rohling et al., 2002; Capotondi et al., 2006.
[d] Based on Emeis et al., 2003.

Mediterranean basin through the Strait of Sicily. Site 969, located on the Mediterranean Ridge at a water depth of 2200 mbsl, represents the centermost location in the Eastern Mediterranean. Sites 966 and 967 are located in the Levantine Basin. Site 967 contains a sequence of deep pelagic sediments (2555 mbsl), but the detrital influence is greater than the previously mentioned sites, since it is influenced by the Nile River plume. Site 966 is situated near Site 967 on a pelagic high, Eratosthenes seamount, at a relatively shallow water depth of 926 mbsl. The sediments in these cores are composed mostly of nannofossil clay, clayey nannofossil ooze and nannofossil ooze with some intervals of clay and foraminifera sand, variably bioturbated (Emeis et al., 1996; Emeis et al., 2000). Dark colored to black sapropel layers appear periodically interbedded with marls. Representative samples were taken at 2 cm resolution from total organic carbon (TOC) enriched sediments and from the overlying and underlying organic-lean sediments in these cores. A finer resolution sampling was carried out close to the contacts between TOC-rich and "background" sediments.

Samples were dried and ground in an agate mortar, homogenized and prepared for geochemical analyses. TOC measurements were done using a *Perkin-Elmer Elemental analyzer* at the Stable Isotope Laboratory (Stanford University), after progressive acidification with cold H_2SO_3 and also at Bremen University, decalcifying with 6 N HCl in excess, using a Heraeus CHN–O-Rapid elemental analyzer. Major elements (Al, Mn) were determined by atomic absorption spectrometry at the Analytical Facilities of the University of Granada. Trace elements were measured with an ICP-MS Perkin-Elmer Sciex Elan 5000 spectrometer (CIC; Analytical Facilities of the University of Granada), using Re and Rh as internal standards. These analyses were carried out after HNO_3 and HF digestion. Coefficients of variation calculated by dissolution and subsequent analyses of 10 replicates of powdered samples were better than 3% and 8% for analyte concentrations of 50 and 5 ppm respectively (Bea, 1996).

From total U and Th concentrations the authigenic U fraction (U_{aut}) has been calculated as $U_{aut} = U_{tot} - Th/3$, (after Wignall and Myers, 1988 see also Jones and Manning, 1994).

Linear sedimentation rates (LSR) were calculated for our particular sampling intervals following two different approaches.

The first one, the "constant LSR assumption", is based on the methodology used by Meyers and Arnaboldi (2005), assuming that the peak TOC concentration measured in each sapropel layer represents the orbitally tuned age of the northern hemisphere insolation maxima with a 3 ky lag. We consider the midpoint of the Ba/Al peak (where sampling allows it), not the TOC increase, since organic carbon is susceptible of post-depositional oxidation, as will be discussed later. The difference in core depths between successive sapropel layers is then divided by ~21 ky of each precessional cycle to obtain LSR and to calculate ages. This model thus implicitly assumes that sediment accumulation rate was identical during sapropel and non-sapropel intervals.

In analogy to observations for S1 sapropel, the second method, the "synchronous sapropel deposition assumption", assumes that base

Fig. 2. Profiles for TOC (%), Ba/Al and Mn/Al ($\times 10^{-4}$), age in vertical scale. Dark grey shading corresponds to visible sapopel, based on TOC concentration and dark colored sediments. Light grey shading represents oxidized sapropel, determined by the offset between Ba/Al and TOC increases. This offset is in some cases indicated also by Mn/Al peaks marking the oxidation fronts. Off-scale values are shown for Mn/Al and Ba/Al.

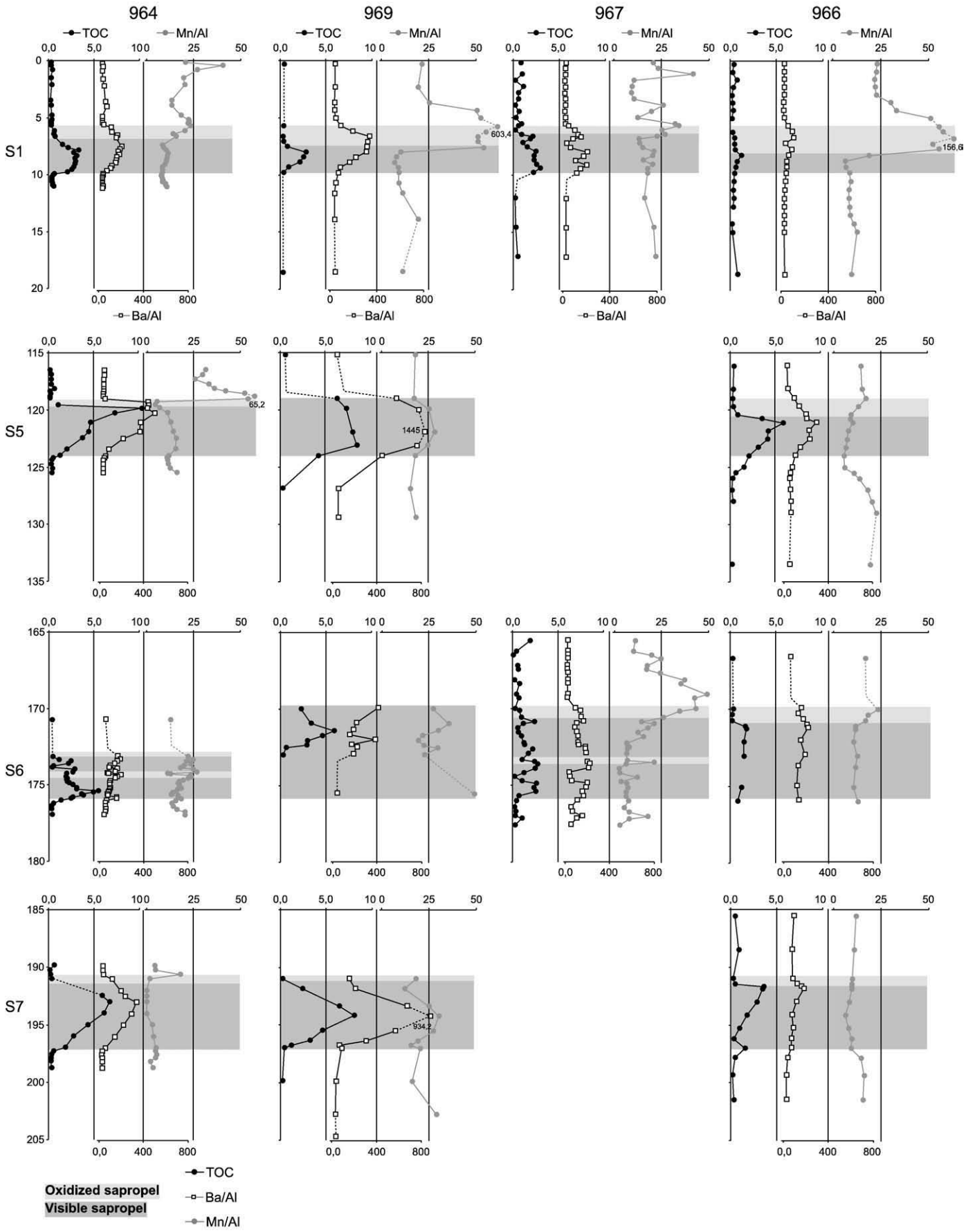
964
969
967
966
TOC
Mn/Al
Ba/Al
S1
S5
S6
S7
603,4
156,6
65,2
1445
934,2
Oxidized sapropel
Visible sapropel
TOC
Ba/Al
Mn/Al

and top for each sapropel are synchronous. Ba/Al and C_{org} are used as an indicator of top and bottom, respectively, of the increased productivity period. It must be noted that some uncertainties occur due to sampling resolution and to ages and duration for sapropels. The ages and duration of each sapropel layer have been taken from previous publications (Emeis et al., 2000; Rohling et al., 2002; Emeis et al., 2003; Capotondi et al., 2006; De Lange et al., 2008) and have been applied to all cores. This duration is then used to calculate LSR within the sapropel for each core. Sedimentation rates above and below the sapropel have been calculated from the depth difference and ages between top and base of adjacent sapropels.

3. Results

3.1. Linear sedimentation rates and sapropel ages

Following the two approaches described above, we obtained very different age models and sedimentation rate estimates. Resulting ages and LSR's obtained following both methods are summarized in Table 2.

For the constant LSR method, the resulting duration of the sapropel event is consistently longer on sites 966 and 969, whereas the shortest events are recorded for the Ionian basin (site 964).

In contrast, for the isochronous sapropel method, the resulting sapropel LSRs are consistently larger than non-sapropel LSRs for sites 966, 967 and 969. Studied sections on site 964 tend to show a decrease in LSRs within the sapropel respect to non-sapropel LSRs, with the exception of S5.

3.2. Geochemical indicators for productivity

Total organic carbon (TOC) in the studied sediments ranges from as low as 0.01% in "background" sediments to 10.3% in Pleistocene sapropel S5 (Fig. 2). As a general trend, higher values are reached in the central and western basins (sites 969 and 964) during sapropel events, whereas slightly to distinctly lower values are observed in the Levantine basin and Eratosthenes seamount respectively. Background sediments generally present values below 0.2%. For all studied sapropels, the highest TOC values are found in S5, for all three sites sampled for that interval. The C_{org} content has a broad general increase in sapropels 1, 5 and 7, but has a complexly fluctuating picture in S6, particularly for sites 964 and 967.

Ba/Al profiles are rather similar to those of TOC, the Ionian basin and the Central Ridge presenting generally higher values than the Levantine basin, and basin-wide maxima occurring during deposition of S5. Although TOC maximum concentrations are slightly higher in the Ionian basin compared to the Mediterranean Ridge (10.31% vs. 8.45%), the Ba/Al ratio behaves oppositely and presents higher values on site 969, up to Ba/Al = 1445, around 3 times the values on site 964. Minor TOC peaks in the upper section of core 967C are not accompanied by a Ba increase. The most pronounced difference between C_{org} and Ba/Al profiles is that in several cases Ba/Al maxima extends to above the C_{org} peak. Where this offset is clearly visible (e.g., S1 basin-wide, or S6 on sites 964 and 966, see Fig. 2) TOC content sharply decreases, whereas Ba/Al maxima progressively return to background values.

3.3. Geochemical indicators for redox conditions

3.3.1. Proxies for oxygen depletion

Trace elements such as Mo, V or U have higher concentrations within sapropel layers, although to a different degree (see Figs. 3 and 4). Sapropel 1 exhibits a moderate Mo enrichment for sites 964 and 967, a minor increase for site 969 and a virtually undetectable maximum for site 966 (Fig. 3). The sapropel deposited during S5 shows a similar Mo/Al ratio for sites 964 and 966, and a slightly higher maximum for site 969 in the center of the basin. Sapropels 6 and 7 have high Mo/Al ratios for site 969, coinciding with enhanced TOC content. For site 964, Mo/Al presents similar values, whereas for the Levantine basin (Sites 966 and 967) this ratio is notably lower. Background sediments generally present a Mo/Al ratio close to 0, with the only exception of sediments around S1 on site 969.

The V/Al ratio presents, as a whole, higher values throughout the studied sections. Profiles are broadly similar to Mo/Al (Fig. 3), although some differences occur. For example, S1 and S5 in the Ionian basin show a double V peak, not identified in the Mo record. In addition, the V/Al ratio is generally more fluctuating within the sapropel. Furthermore, a V increase tends to extend slightly more than the Mo enrichment, (e.g., S6 on site 967 Fig 3, S5 on site 966, S1 on sites 964 and 969).

The authigenic uranium content (U_{aut}; Fig. 4) in sapropel 1 varies from slightly negative values in background sediments up to a 12.1 maximum for site 967, with average values within the sapropel around 4.0 for sites 964 and 969. However, maximum values for site 966 are found below the TOC enriched layer.

U_{aut} in sapropel 5 shows abnormally extreme values for site 969 and generally high levels for the other 2 sampled sites, always coinciding with C_{org}-rich sediments.

The U_{aut} signal in sapropel 6 is very fluctuating for sites 964 and 967, concurring with its TOC content. Maximum values are reached for the Mediterranean Ridge and the deep Levantine basin, while the other 2 locations present maxima below 12.0.

For S7, extreme values of U_{aut} are detected for site 969 also, coinciding with enhanced TOC content. In general, relatively high levels of U_{aut} are reached for the Ionian basin, whereas on top of the Eratosthenes seamount values remain below 12.

V/Mo are plotted as redox "ranges" (Fig. 4), following the intervals described by Piper and Calvert (2009; see below): $V/Mo < 2$ = anoxic; $2 < V/Mo < 10$ = suboxic; $10 < V/Mo < 60$ = oxic; $V/Mo > 60$ = slight dysoxia. V/Mo absolute values generally follow an opposite trend to U_{aut}. Fig. 4). Low values are found coinciding with TOC-rich sediments, background sediments have a $V/Mo \geq 15$ and a sharp increase is clearly observed just above the sapropel level on sites 964 and 967 and it is also distinguishable on the oxidized fronts on sites 966 and 969. This trend is not observed for S1 at site 969, where low values are measured below the sapropel layer, and a minor increase at the top is followed by another minimum. For S1, at the Eratosthenes seamount (966) values remain rather high and stay stable throughout the section, with only a sharp decrease at the top of the visible sapropel. For site 967 a sharp increase is observed in the upper centimeters of the TOC-rich section of S1 sapropel.

3.3.2. Proxies for re-oxygenation

A sharp Mn increase is observed above S1 for all four studied sites (Fig. 2). A similar increase is also detected in some older sapropel layers, although a basin-wide signal is not clear. Distinct Mn peaks are found for the Ionian basin at the top of S5 and S7, for the deep Levantine basin (site 967) at the top of S6, and for the Eratosthenes seamount above S5. Similar increases are not clearly observed in other studied intervals.

3.4. Geochemical signal associated to the sedimentary regime

A decrease in La/Lu is clearly detected during sapropel deposition for the Ionian basin, and this trend is also visible in sapropels S1, S5 and S7 for the Mediterranean Ridge, and for the Eratosthenes seamount in S5 and S7 (Fig. 5). For the deep Levantine basin the contrast of La/Lu between sapropel and non-sapropel sediments is less discernible but can still be detected. Generally, for the Eastern Mediterranean basin, La/Lu values are higher toward the west (sites 969 and 964), where they also become more variable. Non-sapropel sediments at each particular site generally have higher La/Lu ratios than samples corresponding to sapropel layers. Average values of La/

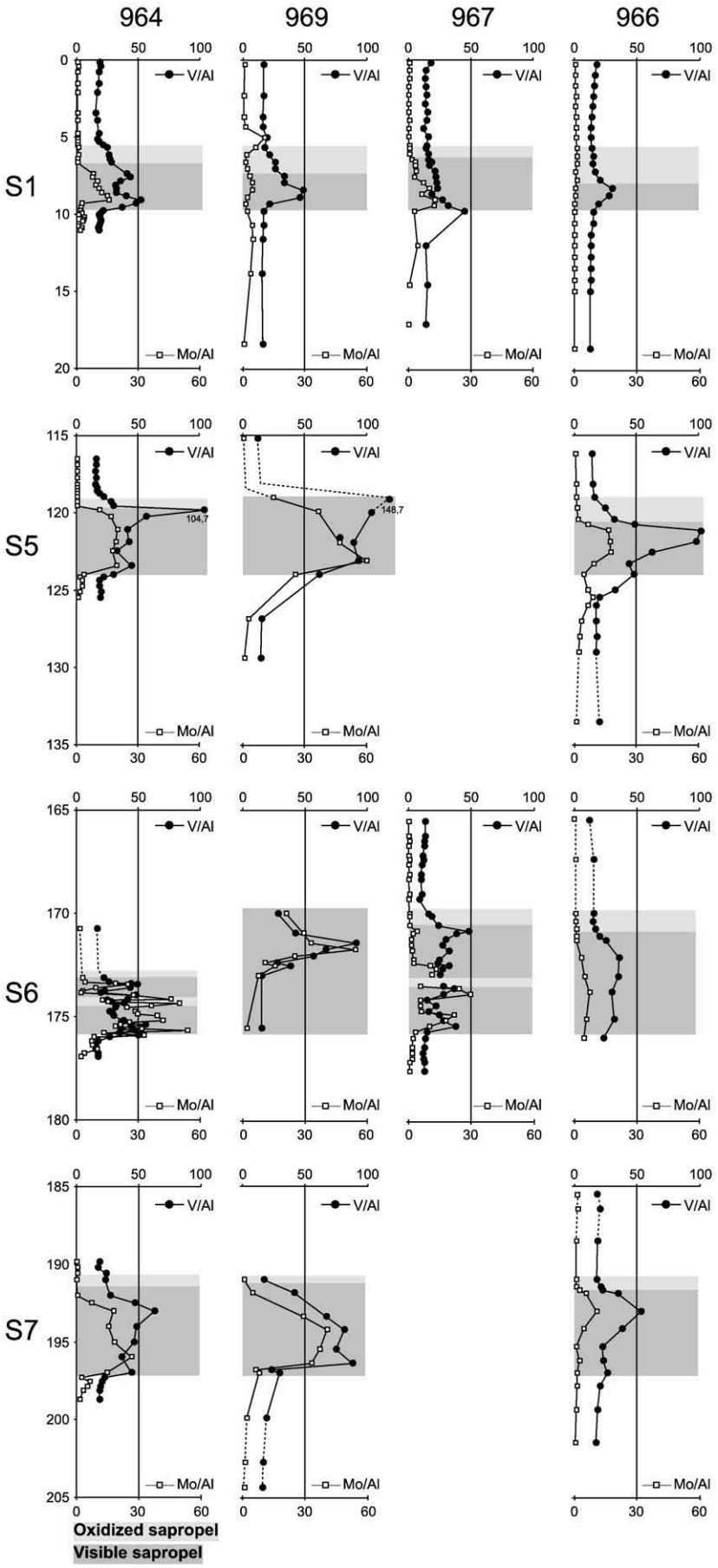

Fig. 3. Profiles for V/Al and Mo/Al ($\times 10^{-4}$). Shading represents the same as in Fig. 2. Note the offset between V/Al and Mo/Al at the top of oxidized sapropels.

Lu for "background" sediments and for each sapropel event are shown in Table 3.

A clear correlation exists between Zr and Hf (Fig. 7) for sites 966 and 967 with a more bimodal pattern for sites 964 and 969. In Fig. 6 we observe the distribution in clusters for each studied site. The two sites located in the Levantine basin tend to plot in the same area more distant to the La/Lu apex, whereas sites 969 and 964 concentrate closer to this apex, defining two clear trend lines.

4. Discussion

The four sites of this study represent not only an East–West transect but also have largely different water depths. In addition, they have variable sedimentation rates and thus potential differences in bio-irrigation and preservation. In particular site 966, being relatively shallow and having low sediment rates, is thought to be most susceptible to mixing and degradation, whereas site 964, being deep and having relatively high sedimentation rates, would be the least susceptible to these processes (Table 2). As a consequence, the latter sediments would be expected to have the most outspoken sapropel features if deepwater stagnation and anoxia would be a dominant control mechanism.

4.1. Age model; isochronous sapropels vs. constant LSRs

Reliable absolute dating, using C^{14} methods, is only available for Sapropel 1 (e.g., De Lange et al., 2008). The ages for all other sapropel layers are assigned based on orbital tuning, paleomagnetic data, and micropaleontological evidence. As a consequence, the age model for all older sapropel units and intercalated sediments depends on several commonly used assumptions, which may lead to some inconsistencies.

If we assume LSRs to remain approximately constant during each individual insolation cycles (e.g., Lourens, 2004; Meyers and Arnaboldi, 2005), thus implicitly assuming that total sedimentation rates for sapropel and non sapropel units are identical, we obtain a clear time difference for the onset and a different duration for each sapropel across the basin (Nijenhuis and De Lange, 2000). The calculated differences range up to 4 ky, (see Table 2-B for details). Similar problems were discussed by Van Os et al. (1994). In particular the shortest sapropel events calculated correspond to the deepest site (964) with the on average highest sedimentation rate. This seems conflicting with the commonly assumed improved organic matter / sapropel preservation under such conditions.

Alternatively, if we assume an isochronous onset and duration of sapropel formation throughout the basin, we can calculate a consistent LSR within each sapropel, but will get a different LSR for "background" sediments between sapropels. Assuming isochronous formation of sapropels seems oceanographically consistent, concordant with basin-wide deepwater ventilation change and enhanced surface waters primary productivity. Alternating periods of inherently different depositional regimes (enhanced and low precipitation and river input, low and high aeolian dust fluxes, enhanced and low primary productivity) would only by coincidence have identical sedimentation rates. Weak points for the isochronous sapropel formation assumption are the age assignments which sometimes cannot be very precise, and the proxy-related sapropel boundary assignments. Possibly as a consequence of this, our resulting different LSRs also show some features that seem contradictory. The variations observed are much larger (Table 2) than reported previously: Nijenhuis and De Lange (2000) suggested maximum LSR variations of 30% lower for non-sapropel sediments or 50% higher during sapropel formation, calculated on the same cores (although on older equivalents). Very high LSR above S1 on site 964 and 967 are not considered reliable due to the possibility of slumped sediments as also evidenced by an additional Mn/Al peak in the upper part of these cores. Finding relatively enhanced sapropel sedimentation rates for those sites that may have been influenced by North African riverine systems (967, 969), and finding the reverse for the site that most likely received its non-biogenic flux from dust (964) is not inconsistent. Therefore, we consider the isochronous sapropel assumption to give the oceanographically most consistent representation for basin-wide sapropel formation, and plots and discussion are elaborated on this option alone.

4.2. Productivity

Increased productivity is thought to be one of the main factors controlling the formation of Eastern Mediterranean sapropels (e.g., Diester-Haass et al., 1998; Martinez-Ruiz et al., 2000; Nijenhuis and De Lange, 2000; Weldeab et al., 2003; Slomp et al., 2004; Meyers and Arnaboldi, 2005). Enhanced export production intensifies the flux of organic matter deposited in the sediments and may exceed the rate of oxidation. In any case, organic matter is easily decomposed and thus a more reliable proxy for increased productivity is needed. Ba-excess (marine barite associated to biogenic activity) has been reported to be a potential productivity proxy (e.g., Bishop, 1988; Dymond et al., 1992; Paytan, 1997), that seems to work particularly well for the most recent S1 sapropel in the Mediterranean region (Van Santvoort et al., 1996; Thomson et al., 1999; Martinez-Ruiz et al., 2000; Rutten and De Lange, 2002; De Lange et al., 2008). The barite marine origin has not only been demonstrated for S1 but also for older units (Paytan et al., 2004). In contrast, serious restrictions have been reported for some other regions and environments of deposition (Francois et al., 1995; McManus et al., 1998; Eagle et al., 2003; Plewa et al., 2006). In summary, although there may be some limitations for its use in older more organic-rich sapropel units (e.g. Van Os et al., 1991), it is still considered a reliable paleo-productivity proxy in a qualitative sense.

All studied intervals show evidence of enhanced productivity during sapropel formation indicated by the increase in Ba/Al ratio, in agreement with previous published studies in the region (e.g., Diester-Haas et al., 1998; Nijenhuis and De Lange, 2000; Weldeab et al., 2003). This increase in surface water productivity and deepwater preservation is the origin of the elevated C_{org} concentrations, although the Ba/Al signal frequently extends for a longer period than TOC (see below). Although Ba-excess cannot always be interpreted quantitatively, (e.g. McManus et al., 1999; Eagle et al., 2003) there is a generally good agreement between enhanced Ba-excess and TOC for each sampled site suggesting a link with surface water productivity. Thus, moderate increases in export productivity were reached during S7 that induced TOC maximum concentrations of around 6% to 7% in the Ionian basin and Mediterranean ridge, and up to 3.6% on top of the Eratosthenes seamount. Sapropel S6 is characterized by a slightly higher surface productivity increase, but under a much stronger sedimentation rate in the Ionian and Levantine basins, so that C_{org} is diluted and lower TOC values are obtained. Substantially stronger is the increase in surface water productivity calculated for S5 and this resulted in maximal TOC concentrations found for this sapropel in all three studied sites. The most recent sapropel formed under moderately high surface productivity conditions and a corresponding moderately high C_{org} content was preserved.

Fig. 4. V/Mo and U_{aut} proxies indicating redox conditions for selected sapropels. Grey shading withing the plots represents V/Mo different ranges of redox condition; $U_{aut} = U_{total} - (Th/3)$ (see text for details). Black dashed line indicate the U_{aut} boundary between low oxygen concentration (>12) and relatively oxic conditions. U_{aut} (linear scale) is merely indicating that redox conditions are within the field of suboxic to anoxic whereas V/Mo (log scale) can make a distiction within that field. By the vertical axis (age) grey bars indicate the period of sapropel formation, including the oxide sapropel (light grey). Dotted and dashed lines of the plots are off-scale values (indicative values are shown).

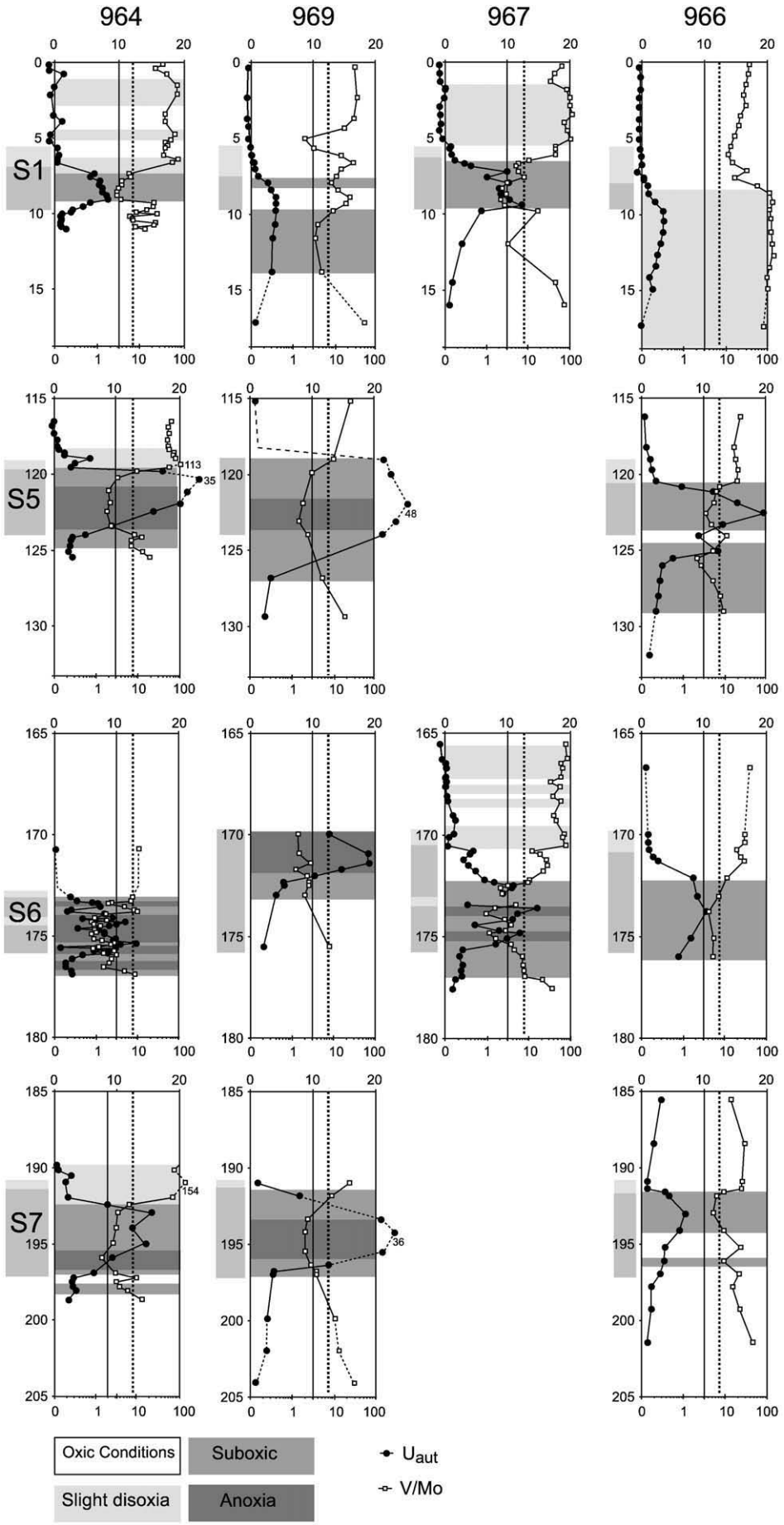
964
969
967
966
S1
S5
S6
S7
113
35
48
154
36
Oxic Conditions
Suboxic
Slight disoxia
Anoxia
Uaut
V/Mo

In summary, enhanced productivity is a requirement for sapropel formation. Later in the discussion we will evaluate the role of deepwater oxygenation in the final sapropel expression and how both factors might be climatically related.

4.3. Redox conditions

One of the continuing discussion points in sapropel formation is whether or not water column anoxia was established during sapropel formation, and as a consequence, if deepwater circulation was stopped or restricted (see Introduction). On the other hand, export productivity might have reached levels that were high enough to produce complete oxygen consumption in the bottom water via organic matter degradation. In any case, changing redox conditions lead to a different geochemical behavior of some diagnostic trace elements (see Introduction).

Trace elements such as Mo, V, U, Cr, etc., are known to precipitate under oxygen-depleted conditions (e.g., Wignall and Myers, 1988; Calvert and Pedersen, 1993; Jones and Manning, 1994; Tribovillard et al., 2006), whereby, as mentioned by Piper and Calvert (2009), the distinction between pore-water and water column anoxia is critical for a correct paleoceanographic interpretation. Different elements precipitate under progressive oxygen depletion; V or U begins to precipitate under suboxic bottom waters whereas Mo or Cu are fixed under fully anoxic environments (see Piper and Calvert, 2009 and references within). This successive element precipitation is the base for calibration of certain redox proxies. One of such proxies is U_{aut} ($U_{aut} = U_{total} - (Th/3)$ where Th is used as a correction for detrital related U; Jones and Manning, 1994). When U_{aut} reaches values >12.0 it is considered to be deposited under anoxic conditions. Another redox proxy V/Mo has been reported to distinguish between suboxic and anoxic conditions: as V starts precipitating under suboxic conditions and Mo only precipitates when dissolved sulphide (H_2S) is available, the ratio V/Mo may distinguish between these two environments (Piper and Isaacs, 1995, 1996). When V/Mo approaches the seawater ratio (<2.0 approx), both metals have precipitated similarly and thus anoxic conditions are inferred. V/Mo between 2 and 10 indicates dysoxic conditions, and between 10 and 50 (approx) it indicates normal oxygenation. When this ratio has anomalously high values (>60) it usually means that V has started to precipitate, but no Mo is yet fixed, thus slightly dysoxic conditions must have prevailed (see also Piper and Calvert, 2009; Piper et al., 2007 and reference therein). The V/Mo values have been plotted as showing these redox condition ranges (Fig. 4). The co-variation of Mo vs. U is also interpreted as indicative of water column dynamics and redox conditions (Algeo and Tribovillard, 2009). It is worth mentioning that none of these proxies should be considered individually since the calibration in terms of oxygen concentration is only an approximation and should not be interpreted quantitatively (see Gallego-Torres et al., 2007).

Each of these elements may also be involved in other processes leading to reduced or enhanced levels, e.g. Mo can be associated to pyrite (e.g. Thomson et al., 1995; Nijenhuis et al., 1999; Siebert et al., 2006; Tribovillard et al., 2006) or to MnO_2 (see below; Reitz et al., 2006), and U can be adsorbed to organic matter (e.g., Baturin, 2002) or downward displaced from an oxidation front (e.g., Colley et al., 1989; Thomson et al., 1995). The ventilation-related upper MnO_2-peak usually encountered above sapropel S1, may contain substantial amounts of Mo (see Reitz et al., 2006). Such enrichment clearly is also the case above S1 at site 969 (Fig. 3), but is not seen in V nor U_{aut}. These observations urge for using multiple proxies; in the following we will use U_{aut} and V/Mo in particular. An additional advantage of the latter proxy is that it consists of elemental ratios thus is insensitive to varying sedimentation rates.

Compelling evidence for S1 indicates that water depth is the dominant factor determining sediment C_{org} content for the deep basin setting (e.g., Murat and Got, 2000; De Lange et al., 2008), which concords with our S1 and S5 data. In contrast, S6 and S7 show higher TOC on the Mediterranean Ridge. Our proxy results indicate that for the studied Pleistocene sapropels, site 969 had the most severely reduced redox depositional conditions. This is consistent with reduced ventilation in the region South of Crete (site 969) and an improved ventilation to the West and East postulated for recent deepwater conditions governed by Adriatic and Aegean outflows (Roether et al., 1996). For site 966, with the most shallow water depth, sapropel redox conditions are generally much less extreme than for the other three sites. If this observed redox variability is entirely attributable to water column oxygenation and redox conditions, then one can make the following deductions:

Sapropel 5 was deposited as a single event and shows the strongest oxygen depletion for the three studied sites, in agreement with previous studies (e.g., Struck et al., 2001; Rohling et al., 2006; Morigi, 2009). Only a short period of anoxia was reached on sites 964 and 969 but relatively minor Mo fixation was observed on site 966, despite being close to anoxic conditions as evidenced by V/Mo. An offset between Mo and V enrichment at the top of the S5 sapropel is evident on all three sites, which indicates a coincident transition through dysoxic conditions across the basin. U_{aut} shows anomalously high values for the central and western basins, always concurrent with C_{org} maxima, probably due to U adsorption to organic matter. Following the interpretation by Algeo and Tribovillard (2009), this anomalous U increase with respect to Mo is also indicating severely diminished bottom water circulation, similar to the present Black Sea situation.

Similar conditions appear to control deposition of S7, although less extreme redox conditions are observed. The end of the “anoxic event” was transitional in the Ionian Basin but more abrupt in the eastern areas, as indicated by V profiles (Fig. 3). The most recent sapropel event (S1) presents a sensibly higher degree of oxygenation across the basin. Only minor oxygen depletion occurred in the Eratosthenes seamount, where in fact the U_{aut} profile extends downward below the sapropel layer, due to U remobilization across the sediment column in the presence of oxygen (Thomson et al., 1987; Colley et al., 1989).

Sapropel 6 is characterized by several pulses of deepwater circulation and/or enhanced productivity, evidenced by intercalated layers of different redox conditions, similar to the profiles of TOC and Ba/Al. Anoxic conditions were thus interrupted by pulses of renewed circulation and/or decreased export productivity and C_{org} flux to the seafloor. In the deep Levantine basin (967) the central part of this sapropel fluctuates between suboxic and anoxic environment whereas the last part corresponds to only suboxic conditions. During S6 suboxic conditions prevailed on the Eratosthenes seamount (966) (both V/Mo and U_{aut} being above the anoxic threshold). Eventual anoxic conditions occurred on site 964 (variable U_{aut}, see Fig. 4), whereas site 969 experienced stable oxygen depletion throughout the event (V/Mo mostly in the anoxic field, Fig. 4) Thus, redox conditions during this sapropel event appear to have been more intense in the western half of the Eastern Mediterranean with a certain West to East gradient. It is worth mentioning that S6 is qualified as “cold sapropel” since it was deposited during a glacial period, and consequently temperature and rainfall, thus water stratification, were lower compared to S5 and S7.

4.4. Post-depositional oxidation

Under oxic conditions, Mn precipitates in the form of oxy-hydroxides. Accordingly, a distinct MnO_2 peak is commonly observed at the sedimentary oxic/suboxic boundary.

Reventilation of the deepwater at the end of sapropel S1 is thought to have resulted in the formation of an upper MnO_2 peak whereas subsequent downward migration of an oxidation front created a lower second MnO_2 peak (e.g. Van Santvoort et al., 1996; Thomson et al., 1999). Such post-depositional oxidation of sapropel S1 has been

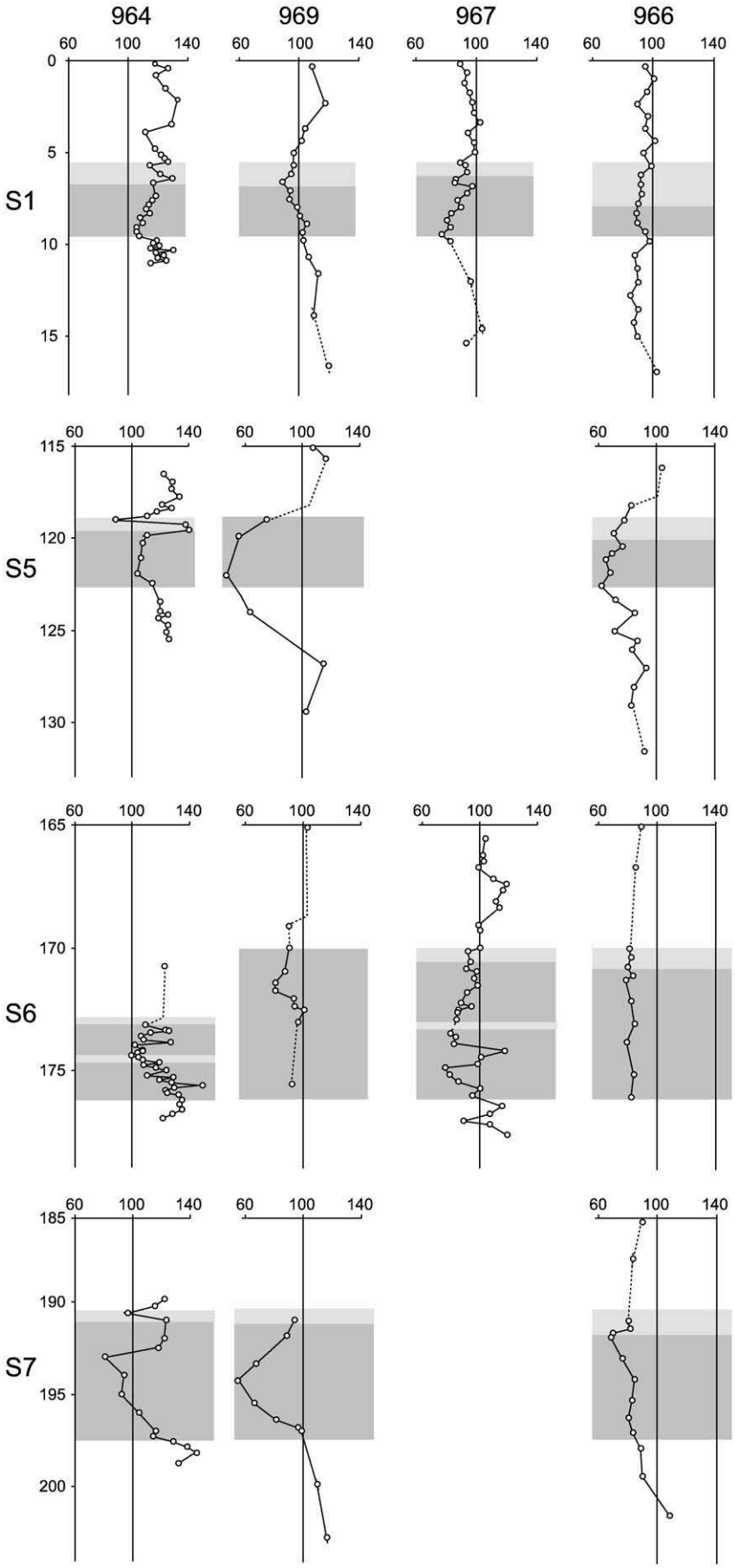

Fig. 5. Profiles for la/Lu indicating variation in the North African area as source of detrital riverine input (Hamroush and Stanley, 1990). Shading represents the same as in Fig. 2.

Table 3
Average La/Lu values for each sapropel event and background sediments.

	Site 964	Site 969	Site 967	Site 966
Background sediments	123,4	107,2	101,6	90,5
S1	113,8	97,5	87,0	92,6
S5	114,7	59,6		71,5
S6	116,5	90,6	91,0	81,5
S7	106,1	80,8		78,4

reported throughout the Eastern Mediterranean (e.g., De Lange et al., 1989; Thomson et al., 1995; Van Santvoort et al., 1996; Martinez-Ruiz et al., 2000; De Lange et al., 2008).

Bottom water re-oxygenation induces oxidation of the organic matter and erases the upper part of the visible sapropel; the Mn increase that defines the so called "burned" sapropel is located at the top of the remaining TOC-rich layer. Our set of data show that this "burn down" of the top centimeters of sapropels has also occurred in Pleistocene equivalents. Moreover, the sharp increase to anomalous high values of V/Mo on top of several sapropel intervals might also be related to this re-oxygenation of bottom waters. When bottom waters become richer in dissolved oxygen Mo is not fixed to the sediment anymore, as described above (offset between Mo and V peaks termination), but is remobilized while V is still stable. Thus, V/Mo ratio sharply increases to anomalous values above normal average values.

The oxidation front is broader and more evident in sapropel 1, and is particularly intense at site 966, where it has nearly obliterated half of the sapropel layer as defined by the enhanced Ba/Al levels.

A thin but intense Mn oxidation front marks the top of S5 in the Ionian basin and the Eratosthenes seamount. This is not visible for S5 on site 969. Similar signs for reventilation/oxidation occur at the top of S7. Fluctuations of TOC content and redox proxy signals are more complex for S6, although a discernible oxidation front appears at the top of this sapropel on the Levantine basin (sites 966 and 967) and within the sapropel (as short interruptions) in the Ionian basin (site 964) and site 967, again coinciding with a sharp increase in V/Mo.

We thus infer that sapropel termination was more abrupt in the two areas where post-depositional oxidation is more evident and frequent, (Levantine and Ionian basins). This reventilation may be related to deepwater fluxes flowing from the Aegean and Adriatic Seas (e.g., Roether et al., 1996). This means that the outflow from these northern areas, that are presently sourcing the deepwater flow in the Eastern Mediterranean, were partly responsible for sapropel termination. At the same time a reduced input of these deep currents might have helped to sustain sapropel formation.

In summary, for those intervals sampled at sufficient resolution, there is clear evidence for a ventilation/re-oxygenation of the deepwater at the end of all studied sapropels but most explicitly retained and visible for the most recent S1 sapropel.

4.5. Sedimentary regime

Using La/Lu ratio, Hf vs. Zr correlation, variations in the source of detrital input to the different basins and the contrast in the sedimentary regime between sapropel events and background sediments can be assessed (Figs. 5–7). La/Lu ratio has been used previously as a proxy for North African craton sediment provenance in the Mediterranean region (e.g., Hamroush and Stanley, 1990; Gallego-Torres et al., 2007), since sediments originating from the Ethiopian plateau and the North African region exhibit a lower La/Lu ratio than those from the central Africa craton due to the different composition of crystalline rocks for each region. The North African region is currently a dry tropical area but was particularly affected by the intensified monsoonal activity during isolation maxima that coincides with sapropel events (e.g., Rossignol-Strick, 1985; Rohling et al., 2002). During the latter period these areas were intensively eroded and provide a major source of riverine detrital sediments, thus shifting the geochemical signal to lower La/Lu values. Hf and Zr have a very similar crystallographic behavior and represent the lithogenous source, so their relation serves to determine if a unique or a variable source of sediments feed each particular site or sub-basin (see Piper and Calvert, 2009). Detrital input in the basin is derived mainly from the rivers draining the northern margin, and through the Nile River and aeolian input of Saharan dust from the south. The latter has been reported to be the major source of terrigenous material at present day and previous arid precession periods (e.g., Wehausen and Brumsack, 1999; Rutten et al., 2000; Weldeab et al., 2002; Jilbert et al., 2010).

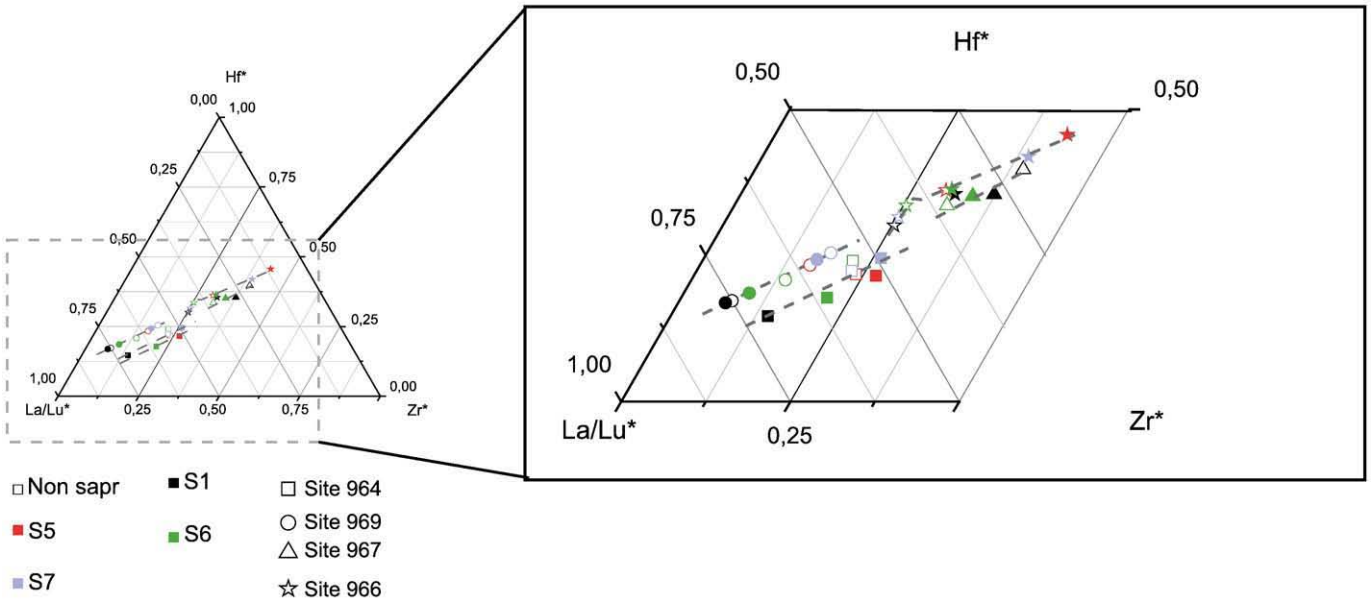

Fig. 6. Distribution of sapropel and non-sapropel sediment as a function of La/Lu, Hf and Zr variations. Elements concentration and La/Lu ratio are normalized as $E^* = {}^{(E\text{me} - E\text{min})}/_{E\text{max} - E\text{min}}$. Each site is indicated by a symbol code and each sapropel is characterized by a color code. Samples from each site cluster along a trend line. Certain sapropel points deviates from the trend, (see text for details).

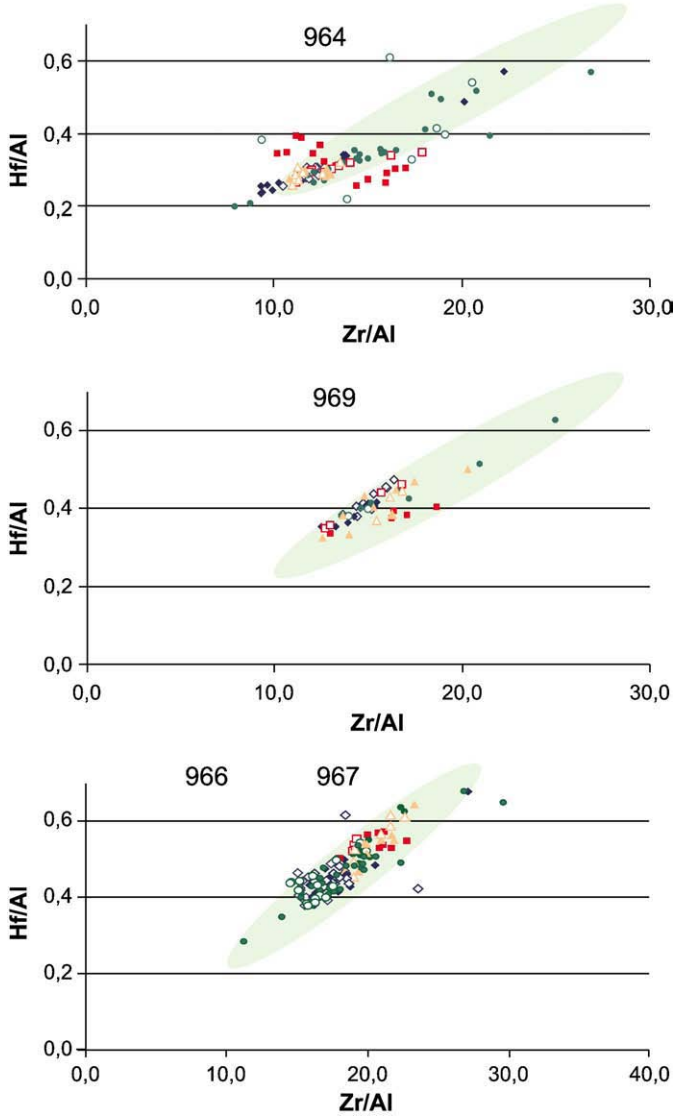

Fig. 7. Correlation between Hf and Zr, related to the sources off detrital input. Full symbols shows background sediments. Each color represents one sapropel event; blue = S1; red = S5; green = S6; orange = S7.

However, during insolation maxima (thus, during sapropel deposition) a more intense rainfall and the northward shift of monsoonal activity in the African continent was likely to induce a change in the sedimentary regime, increasing riverine derived terrigenous material and limiting aeolian supply (e.g., Rossignol-Strick, 1985; Weldeab et al., 2002; Tzedakis, 2007). Our data are consistent with potential active rivers other than the Nile draining the tropical African region during these periods (e.g., Pachur and Kröpelin, 1987; Rohling et al., 2002; Tzedakis, 2007).

La/Lu values are notably lower for the two sites located in the Levantine basin, which is consistent with their proximity to the Nile River outflow. Their detrital material is mostly sourced from the African continent and their variations in La/Lu is thought to respond to fluctuations in abundance of fluvial material transported by the Blue Nile (from the Ethiopian plateau) with respect to central Africa and aeolian input. All studied layers (with the exception of S1 at site 966) present higher input derived from drainage of the tropical African region, evidenced by lower La/Lu (see Figs. 5 and 6).

Site 966, being on a pelagic high, has relatively low sedimentation rates, receives less fluvial detrital material and is thus more influenced by aeolian supply. Bioturbation at this site is also frequent and can make the signal less distinct. In contrast to this trend, site 967 (in the deep Levantine basin), with higher sedimentation rates (see Table 2), is largely influenced by Nile River dynamics and fluctuations and coherently shows large shifts in La/Lu signal. At the western extreme of the Eastern Mediteranean, site 964 shows the highest La/Lu values and limited variation (see Table 3 and Fig. 6). We consider this difference to be related to alternative sources of detrital material, such as from the Adriatic Sea and Sicily. Consistently low La/Lu values during sapropel deposition in the central ridge (site 969) evidences an intense southern sediment provenance (although not unique, as explained below), either sourced by the Nile River or other active North Africa river.

The most intense La/Lu signal for tropical African drainage occurs during deposition of sapropels 5 and 7 (see Table 3), inferring a particularly strong monsoonal activity and a large volume of detrital material and thus riverwater from this area. Minimum influence is observed for S1 and S6.

Since detrital material on sites 966 and 967 are mostly sourced from the same area along all studied periods, Zr/Hf behaves following a constant and coherent trend (see Fig. 7), whereas sites 969 and 964 present deviations from this pattern because they both receive input from other sources, namely the northern margins or ancient southern river systems other than the Nile. For these two sites, deviations from the main trend correspond to samples from sapropel 5 and, locally from S6 and S7 indicating variable sources. S5 and S7 appear to be particularly influenced by an intense input of detrital material from the African tropical region and this deviation is coherent with that interpretation. In the case of S6, Zr/Hf shows a more scattered distribution (see Fig. 7, site 964). This event occurred during a relatively cold period and thus we may expect less intense monsoonal activity in tropical Africa, a weaker riverine input from the south (compared to other sapropel events) and a stronger outflow from the European margins. Besides, this sapropel event presents several internal fluctuations and thus intermittent input of detrital material from different sources is expected.

It seems therefore, that the more intense sapropel events (S5 and S7) occurred under higher influence of drainage from the area strongly eroded by the intensified African monsoon. This might have prevented normal circulation and resulted in more extreme deepwater oxygen depletion (stagnation) and intensification of surface productivity, thus higher TOC content. The relatively poorly developed sapropel 1 received much less input from the southern margin, similar to S6 (a "cold" sapropel) which was most likely more influenced by northern margin drainage and thus developed more intensely in the western basin.

Integrating our proxy-based findings on paleoceanographic conditions and on the origin of terrestrial material leads to a few interesting interpretations: deepwater formation, originating from Adriatic and Aegean regions, indirectly determines deepwater ventilation and oxygenation, thus the time interval of sapropel accumulation. The more extreme sapropel events concur with more extreme monsoon-associated run of from North Africa. In other words, extremes in North African monsoonal activity appear to control the intensity of sapropel events in the Eastern Mediterranean. On the other hand, deepwater flux from the northern areas, particularly the Adriatic and Aegean seas, controlled the termination of each sapropel event and maybe some internal features such as the interruption during S1 (e.g. Rohling et al., 1997; De Rijk et al., 1999; Gennari et al., 2009) or the fluctuations observed on S7 (Fig. 3).

5. Conclusions: conditions for sapropel formation

Sapropel formation derives from the combination of enhanced surface productivity and bottom water stagnation. Sapropels deposited during warm periods (S5 and S7) formed under an intensified

influence from riverine input sourced from the African tropical region, and thus enhanced fluvial run-off related to monsoonal activity in that area. This intense input from the south is not so evident for S6, deposited during a cold period. In this case, a source from the northern continent is more likely, but this input was highly fluctuating and sapropel formation responded to these pulses by intermittent deposition.

Analogue to recent observations, Adriatic and Aegean seas are thought to have been the source areas for deepwater outflow into the Eastern Mediterranean. Climatic conditions on the northern margin of the region control the deepwater outflow which substantially contributes to deepwater ventilation. At the same time, the termination of sapropel formation is defined by this deepwater formation.

Oxygen depletion in the water column was achieved to a different extent during sapropel formation. Maximum extension of water column anoxia was achieved during S5 deposition, where even the Eratosthenes seamount achieved notable dysoxia. Redox-related trace element patterns indicate that S5 and S7 are the most intense sapropels; these intervals are also the most extreme in monsoonal activity in tropical Africa and thus drainage, as deduced from our La/Lu and Zr/Hf patterns. This indicates that extremes in African monsoonal activity determine the intensity of sapropel formation.

Acknowledgments

We would like to thank Projects MARM 200800050084447, MICINN CGL2009-07603 from the Ministerio de Ciencia y Tecnologia, the Research Group Junta de Andalucía RNM-5212, and Plan Propio de Investigación (UGR) for their financial support. We also thank the Centro de Instrumentación Cientifica (UGR) for their analytical work. We are grateful to two anonymous reviewers for their constructive comments. We are grateful to the Ocean Drilling Program for providing us with the samples used in this study as well as to the ODP Core Repository (Bremen, Germany) for assistance with sampling.

References

Algeo, T.J., Tribovillard, N., 2009. Environmental analysis of paleoceanographic systems based on molybdenum–uranium covariation. Chemical Geology 268 (3–4), 211–225.

Arnaboldi, M., Meyers, P.A., 2006. Patterns of organic carbon and nitrogen isotopic compositions of latest Pliocene sapropels from six locations across the Mediterranean Sea. Palaeogeography, Palaeoclimatology, Palaeoecology 235 (1–3), 149–167.

Baturin, G.N., 2002. Uranium and phosphorus in deep-sea clay from the Pacific Ocean. Oceanology 42 (5), 723–730.

Bea, F., 1996. Residence of REE, Y, Th and U in granites and crustal protoliths: implications for the chemistry of crustal melts. Journal of Petrology 37, 521–532.

Bishop, J.K.B., 1988. The barite–opal–organic carbon association in oceanic particulate matter. Nature 332, 341–343.

Calvert, S.E., Pedersen, T.F., 1993. Geochemistry of Recent oxic and anoxic marine sediments: Implications for the geological record. Marine Geology 113 (1–2), 67–88.

Calvert, S.E., Nielsen, B., Fontugne, M.R., 1992. Evidence from nitrogen isotope ratios for enhanced productivity during formation of Eastern Mediterranean sapropels. Nature 359 (6392), 223–225.

Capotondi, L., Principato, M.S., Morigi, C., Sangiorgi, F., Maffioli, P., Giunta, S., Negri, A., Corselli, C., 2006. Foraminiferal variations and stratigraphic implications to the deposition of sapropel S5 in the eastern Mediterranean. Palaeogeography, Palaeoclimatology, Palaeoecology 235 (1–3), 48–65.

Cita, M.B., Vergnaud-Grazzini, C., Robert, C., Chamley, H., Ciaranfi, N., d'Onofrio, S., 1977. Paleoclimatic record of a long deep sea core from the eastern Mediterranean. Quaternary Research 8 (2), 205–235.

Colley, S., Thomson, J., Toole, J., 1989. Uranium relocations and derivation of quasi-isochronon for a turbidite pelagic sequence in the Northeast Atlantic. Geochimica et Cosmochimica Acta 53 (6), 1223–1234.

Crusius, J., Thomson, J., 2003. Mobility of authigenic rhenium, silver, and selenium during postdepositional oxidation in marine sediments. Geochimica et Cosmochimica Acta 67 (2), 265–273.

De Lange, G.J., Ten Haven, H.L., 1983. Recent sapropel formation in the Eastern Mediterranean. Nature 305, 797–798.

De Lange, G.J., Middelburg, J.J., Pruysers, P.A., 1989. Discussion: Middle and Late Quaternary depositional sequences and cycles in the eastern Mediterranean. Sedimentology 36, 151–156.

De Lange, G.J., Thomson, J., Reitz, A., Slomp, C.P., Principato, M.S., Erba, E., Corselli, C., 2008. Synchronous basin-wide formation and redox-controlled preservation of a Mediterranean sapropel. Nature Geosciences 1 (9), 606–610.

De Rijk, S., Hayes, A., Rohling, E.J., 1999. Eastern Mediterranean sapropel S1 interruption: an expression of the onset of climatic deterioration around 7 ka BP. Marine Geology 153 (1–4), 337–343.

Diester-Haass, L., Robert, C., Chamley, H., 1998. Paleoproductivity and climate variations during sapropel deposition in the Eastern Mediterranean Sea. In: Robertson, A.H.F., Emeis, K.-C., Richter, C., Camerlenghi, A. (Eds.), Proceedings of Ocean Drilling Program, Scientific Results, pp. 227–248.

Dymond, J., Suess, E., Lyle, M., 1992. Barium in deep-sea sediment: a geochemical proxy for paleoproductivity. Paleoceanography 7, 163–181.

Eagle, M., Paytan, A., Arrigo, K.R., van Dijken, G., Murray, R.W., 2003. A comparison between excess barium and barite as indicators of carbon export. Paleoceanography 18 (1).

Emeis, K.-C., Camerlenghi, A., McKenzie, J.A., Rio, D., Sprovieri, R., 1991. The occurrence and significance of Pleistocene and Upper Pliocene sapropels in the Tyrrhenian Sea. Marine Geology 100 (1–4), 155–182.

Emeis, K.C., Robertson, A.H.F., Ritcher, C.e.a., 1996. Proceedings of the ocean drilling program: Initial Reports, Vol. 160, p. 160.

Emeis, K.-C., Sakamoto, T., Wehausen, R., Brumsack, H.-J., 2000. The sapropel record of the eastern Mediterranean Sea — results of Ocean Drilling Program Leg 160. Palaeogeography, Palaeoclimatology, Palaeoecology 158 (3–4), 371–395.

Emeis, K.C., Schulz, H., Struck, U., Rossignol-Strick, M., Erlenkeuser, H., Howell, M.W., Kroon, D., Mackensen, A., Ishizuka, S., Oba, T., Sakamoto, T., Koizumi, I., 2003. Eastern Mediterranean surface water temperatures and delta O-18 composition during deposition of sapropels in the late Quaternary. Paleoceanography 18 (1).

Filippelli, G.M., Sierro, F.J., Flores, J.A., Vazquez, A., Utrilla, R., Perez-Folgado, M., Latimer, J.C., 2003. A sediment–nutrient–oxygen feedback responsible for productivity variations in Late Miocene sapropel sequences of the western Mediterranean. Palaeogeography, Palaeoclimatology, Palaeoecology 190, 335–348.

Francois, R., Honjo, S., Manganini, S.J., Ravizza, G.E., 1995. Biogenic barium fluxes to the deep-sea — implications for paleoproductivity reconstruction. Global Biogeochemical Cycles 9 (2), 289–303.

Gallego-Torres, D., Martinez-Ruiz, F., Paytan, A., Jimenez-Espejo, F.J., Ortega-Huertas, M., 2007. Pliocene–Holocene evolution of depositional conditions in the eastern Mediterranean: role of anoxia vs. productivity at time of sapropel deposition. Palaeogeography, Palaeoclimatology, Palaeoecology 246 (2–6), 424–439.

Gennari, G., Tamburini, F., Ariztegui, D., Hajdas, I., Spezzaferri, S., 2009. Geochemical evidence for high-resolution variations during deposition of the Holocene S1 sapropel on the Cretan Ridge. Eastern Mediterranean, Palaeogeography, Palaeoclimatology, Palaeoecology 273, 239–248.

Hamroush, H.A., Stanley, a.D.J., 1990. Paleoclimatic oscillations in East Africa interpreed by analysis of trace elements in Nile delta sediments. Episodes 13, 264–269.

Hilgen, F.J., 1991. Astronomical calibration of Gauss to Matuyama sapropels in the Mediterranean and implication for the Geomagnetic Polarity Time Scale. Earth and Planetary Science Letters 104 (2–4), 226–244.

Jilbert, T., Reichart, G.J., Aeschlimann, B., Gunther, D., Boer, W., de Lange, G., 2010. Climate-controlled multidecadal variability in North African dust transport to the Mediterranean. Geology 38, 19–22.

Jones, B.A., Manning, D.A.C., 1994. Comparison of geochemical indices used for the interpretation of palaeoredox conditions in ancient mudstones. Chemical Geology 111, 111–129.

Kidd, R.B., Cita, M.B., Ryan, W.B.F., 1978. Stratigraphy of eastern Mediterranean sapropel sequences recovered during Leg 42 A and their paleoenvironmental significance. Initial report DSDP, pp. 421–443.

Lourens, L.J., 2004. Revised tuning of Ocean Drilling Program Site 964 and KC01B (Mediterranean) and implications for the delta O-18, tephra, calcareous nannofossil, and geomagnetic reversal chronologies of the past 1.1 Myr. Paleoceanography 19 (3).

Martinez-Ruiz, F., Kastner, M., Paytan, A., Ortega-Huertas, M., Bernasconi, S.M., 2000. Geochemical evidence for enhanced productivity during S1 sapropel deposition in the eastern Mediterranean. Paleoceanography 15 (2), 200–209.

Martinez-Ruiz, F., Paytan, A., Kastner, M., Gonzalez-Donoso, J.M., Linares, D., Bernasconi, S.M., Jimenez-Espejo, F.J., 2003. A comparative study of the geochemical and mineralogical characteristics of the S1 sapropel in the western and eastern Mediterranean. Palaeogeography, Palaeoclimatology, Palaeoecology 190, 23–37.

McManus, J., Berelson, W.M., Klinkhammer, G.P., Johnson, K.S., Coale, K.H., Anderson, R.F., Kumar, N., Burdige, D.J., Hammond, D.E., Brumsack, H.J., McCorkle, D.C., Rushdi, A., 1998. Geochemistry of barium in marine sediments: Implications for its use as a paleoproxy. Geochimica et Cosmochimica Acta 62 (21–22), 3453–3473.

McManus, J., Berelson, W.M., Hammond, D.E., Klinkhammer, G.P., 1999. Barium cycling in the North Pacific: implications for the utility of Ba as a paleoproductivity and paleoalkalinity proxy. Paleoceanography 14 (1), 53–61.

Menzel, D., Hopmans, E.C., van Bergen, P.F., de Leeuw, J.W., Sinninghe Damste, J.S., 2002. Development of photic zone euxinia in the eastern Mediterranean Basin during deposition of Pliocene sapropels. Marine Geology 189 (3–4), 215–226.

Menzel, D., van Bergen, P.F., Schouten, S., Sinninghe Damste, J.S., 2003. Reconstruction of changes in export productivity during Pliocene sapropel deposition: a biomarker approach. Palaeogeography, Palaeoclimatology, Palaeoecology 190, 273–287.

Meyers, P.A., Arnaboldi, M., 2005. Trans-Mediterranean comparison of geochemical paleoproductivity proxies in a mid-Pleistocene interrupted sapropel. Palaeogeography, Palaeoclimatology, Palaeoecology 222 (3–4), 313–328.
Morigi, C., 2009. Benthic environmental changes in the Eastern Mediterranean Sea during sapropel S5 deposition. Palaeogeography, Palaeoclimatology, Palaeoecology 273 (3–4), 258–271.
Murat, A., Got, H., 2000. Organic carbon variations of the eastern Mediterranean Holocene sapropel: a key for understanding formation processes. Palaeogeography, Palaeoclimatology, Palaeoecology 158 (3–4), 241–257.
Negri, A., Morigi, C., Giunta, S., 2003. Are productivity and stratification important to sapropel deposition? Microfossil evidence from late Pliocene insolation cycle 180 at Vrica, Calabria. Palaeogeography, Palaeoclimatology, Palaeoecology 190, 243–255.
Nijenhuis, I.A., De Lange, G.J., 2000. Geochemical constraints on Pliocene sapropel formation in the eastern Mediterranean. Marine Geology 163 (1–4), 41–63.
Nijenhuis, I.A., Bosch, H.-J., Sinninghe Damste, J.S., Brumsack, H.-J., De Lange, G.J., 1999. Organic matter and trace element rich sapropels and black shales: a geochemical comparison. Earth and Planetary Science Letters 169 (3–4), 277–290.
Nijenhuis, I.A., Becker, J., De Lange, G.J., 2001. Geochemistry of coeval marine sediments in Mediterranean ODP cores and a land section: implications for sapropel formation models. Palaeogeography, Palaeoclimatology, Palaeoecology 165 (1–2), 97–112.
Olausson, E., 1961. Studies of deep-sea cores. Report of Swedish Deep-sea Expeditions, 1947–48 8, pp. 337–391.
Pachur, H.J., Kröpelin, S., 1987. Wadi Howar: paleoclimatic evidence from an extinct river system in the Southeastern Sahara. Science 237 (4812), 298–300.
Passier, H.F., Middelburg, J.J., De Lange, G.J., Bottcher, M.E., 1999. Modes of sapropel formation in the eastern Mediterranean: some constraints based on pyrite properties. Marine Geology 153 (1–4), 199–219.
Paytan, A., 1997. Marine barite, a recorder of oceanic chemistry, productivity, and circulation., La Jolla, California, La Jolla, 111 pp.
Paytan, A., Martinez-Ruiz, F., Eagle, M., Ivy, A., Wankel, S.D., 2004. Using sulfur isotopes in barite to elucidate the origin of high organic matter accumulation events in marine sediments. Sulfur Biogeochemistry, GSA Special Paper 379, 151–160.
Piper, D.Z., Calvert, S.E., 2009. A marine biogeochemical perspective on black shale deposition. Earth Science Reviews 95 (1–2), 63–96.
Piper, D.Z., Isaacs, C.M., 1995. Minor elements in Quaternary sediments from the sea of Japan — a record for surface-water productivity and intermediate-water redox conditions. Geological Society of America Bulletin 107 (1), 54–67.
Piper, D.Z., Isaacs, C.M., 1996. Instability of bottom-water redox conditions during accumulation of quaternary sediment in the Japan Sea. Paleoceanography 11 (2), 171–190.
Piper, D.Z., Perkins, R.B., Rowe, H.D., 2007. Rare-earth elements in the Permian Phosphoria Formation: paleo proxies of ocean geochemistry. Deep-Sea Researcht Part II 54 (11–13), 1396–1413.
Plewa, K., Meggers, H., Kasten, S., 2006. Barium in sediments off northwest Africa: a tracer for paleoproductivity or meltwater events? Paleoceanography 21 (2).
Reitz, A., Thomson, J., De Lange, G.J., Green, D.R.H., Slomp, C.P., Gebhardt, A.C., 2006. Effects of the Santorini (Thera) eruption on manganese behavior in Holocene sediments of the eastern Mediterranean. Earth and Planetary Science Letters 241 (1–2), 188–201.
Rinna, J., Warning, B., Meyers, P.A., Brumsack, H.J., Rullkotter, J., 2002. Combined organic and inorganic geochemical reconstruction of paleodepositional conditions of a Pliocene sapropel from the eastern Mediterranean Sea. Geochimica et Cosmochimica Acta 66 (11), 1969–1986.
Roether, W., Manca, B.B., Klein, B., Bregant, D., Georgopoulos, D., Beitzel, V., Kovacevic, V., Luchetta, A., 1996. Recent changes in eastern Mediterranean deep waters. Science 271 (5247), 333–335.
Rohling, E.J., Hilgen, F.J., 1991. The Eastern Mediterranean climate at times of sapropel formation — a review. Geologie en Mijnbouw 70 (3), 253–264.
Rohling, E.J., Jorissen, F.J., De Stigter, H.C., 1997. 200 year interruption of Holocene sapropel formation in the Adriatic Sea. Journal of Micropalaeontology 16 (2), 97–108.
Rohling, E.J., Cane, T.R., Cooke, S., Sprovieri, M., Bouloubassi, I., Emeis, K.C., Schiebel, R., Kroon, D., Jorissen, F.J., Lorre, A., Kemp, A.E.S., 2002. African monsoon variability during the previous interglacial maximum. Earth and Planetary Science Letters 202 (1), 61–75.
Rohling, E.J., Hopmans, E.C., Damste, J.S.S., 2006. Water column dynamics during the last interglacial anoxic event in the Mediterranean (sapropel S5). Paleoceanography 21 (2).
Rossignol-Strick, M., 1985. Mediterranean Quaternary sapropels, an immediate response of the African monsoon to variation of insolation. Palaeogeography, Palaeoclimatology, Palaeoecology 49 (3–4), 237–263.
Rutten, A., De Lange, G.J., 2002. A novel selective extraction of barite, and its application to eastern Mediterranean sediments. Earth and Planetary Science Letters 198 (1–2), 11–24.
Rutten, A., De Lange, G.J., Ziveri, P., Thomson, J., van Santvoort, P.J.M., Colley, S., Corselli, C., 2000. Recent terrestrial and carbonate fluxes in the pelagic eastern Mediterranean; a comparison between sediment trap and surface sediment. Palaeogeography, Palaeoclimatology, Palaeoecology 158 (3–4), 197–213.
Sakamoto, T., Janecek, T., Emeis, K.C., 1999. Continuous sedimentary sequences from the eastern Mediterranean Sea: composite depth sections. Proceedings of the Ocean Drilling Program: Scientific Results 160, 37–60.
Siebert, C., McManus, J., Bice, A., Poulson, R., Berelson, W.M., 2006. Molybdenum isotope signatures in continental margin marine sediments. Earth and Planetary Science Letters 241 (3–4), 723–733.
Slomp, C.P., Thomson, J., De Lange, G.J., 2004. Controls on phosphorus regeneration and burial during formation of eastern Mediterranean sapropels. Marine Geology 203 (1–2), 141–159.
Struck, U., Emeis, K.-C., Vo[ss], M., Krom, M.D., Rau, G.H., 2001. Biological productivity during sapropel S5 formation in the Eastern Mediterranean Sea: evidence from stable isotopes of nitrogen and carbon. Geochimica et Cosmochimica Acta 65 (19), 3249–3266.
Thomson, J., Colley, S., Higgs, N.C., Hydes, D.J., Wilson, T.R.S., 1987. Geochemical oxidation fronts in NE Atlantic distal turbidites and their effects in the sedimentary record. In: Weaver, P.P.E., Thomson, J. (Eds.), Geology and Geochemistry of Abyssal Plains. Geological Society of London, pp. 167–177.
Thomson, J., Higgs, N.C., Wilson, T.R.S., Croudace, I.W., De Lange, G.J., Van Santvoort, P.J.M., 1995. Redistribution and geochemical behaviour of redox-sensitive elements around S1, the most recent eastern Mediterranean sapropel. Geochimica et Cosmochimica Acta 59 (17), 3487–3501.
Thomson, J., Mercone, D., De Lange, G.J., Van Santvoort, P.J.M., 1999. Review of recent advances in the interpretation of eastern Mediterranean sapropel S1 from geochemical evidence. Marine Geology 153 (1–4), 77–89.
Thunell, R.C., Williams, D.F., Belyea, P.R., 1984. Anoxic events in the Mediterranean Sea in relation to the evolution of late Neogene climates. Marine Geology 59 (1–4), 105–134.
Tribovillard, N., Algeo, T.J., Lyons, T., Riboulleau, A., 2006. Trace metals as paleoredox and paleoproductivity proxies: an update. Chemical Geology 232 (1–2), 12–32.
Tzedakis, P.C., 2007. Seven ambiguities in the Mediterranean palaeoenvironmental narrative. Quaternary Science Reviews 26 (17–18), 2042–2066.
Van Os, B.J.H., Middelburg, J.J., De Lange, G.J., 1991. Possible diagenetic mobilization of barium in sapropelic sediment from the eastern Mediterranean. Marine Geology 100 (1–4), 125–136.
Van Os, B.J.H., Lourens, L.J., Hilgen, F.J., De Lange, G.J., Beaufort, L., 1994. The formation of Pliocene sapropels and carbonate cycles in the Mediterranean: diagenesis, dilution, and productivity. Paleoceanography 9 (4), 601–617.
Van Santvoort, P.J.M., De Lange, G.J., Thomson, J., Cussen, H., Wilson, T.R.S., Krom, M.D., Strohle, K., 1996. Active post-depositional oxidation of the most recent sapropel (S1) in sediments of the eastern Mediterranean Sea. Geochimica et Cosmochimica Acta 60 (21), 4007–4024.
Wehausen, R., Brumsack, H.-J., 1999. Cyclic variations in the chemical composition of eastern Mediterranean Pliocene sediments: a key for understanding sapropel formation. Marine Geology 153 (1–4), 161–176.
Weldeab, S., Emeis, K.-C., Hemleben, C., Siebel, W., 2002. Provenance of lithogenic surface sediments and pathways of riverine suspended matter in the Eastern Mediterranean Sea: evidence from 143Nd/144Nd and 87Sr/86Sr ratios. Chemical Geology 186 (1–2), 139–149.
Weldeab, S., Emeis, K.-C., Hemleben, C., Schmiedl, G., Schulz, H., 2003. Spatial productivity variations during formation of sapropels S5 and S6 in the Mediterranean Sea: evidence from Ba contents. Palaeogeography, Palaeoclimatology, Palaeoecology 191 (2), 169–190.
Wignall, P.B., Myers, K.J., 1988. Interpreting the benthic oxygen levels in mudrocks: a new approach. Geology 16, 452–455.